Dalton Transactions

PAPER

View Article Online
View Journal | View Issue

The energy transfer and effect of doped Mg^{2+} in $Ca_3Sc_2Si_3O_{12}:Ce^{3+}$, Pr^{3+} phosphor for white LEDs

Cite this: *Dalton Trans.*, 2014, **43**, 4146

Jun Qiao,[a,b] Jiahua Zhang,*[a] Xia Zhang,[a] Zhendong Hao,[a] Yongfu Liu[a] and Yongshi Luo[a]

Received 15th October 2013,
Accepted 21st November 2013

DOI: 10.1039/c3dt52902a

www.rsc.org/dalton

The energy transfer and luminescence properties in the Ce^{3+} and Pr^{3+} co-activated $Ca_3Sc_2Si_3O_{12}$ (CSS) silicate garnet are studied in our work. The addition of Pr^{3+} exhibits a red emission around 610 nm in the green phosphor CSS:Ce^{3+}, but the amount of Pr^{3+} incorporated into the phosphor is very limited due to the charge mismatch when Pr^{3+} substitutes for Ca^{2+} in CSS. In order to promote Pr^{3+} incorporation into CSS lattices to enhance the red emission component, the addition of Mg^{2+} incorporated into Sc^{3+} site is performed to compensate the residual positive charge caused by the substitution of Pr^{3+} for Ca^{2+} in CSS. Finally, a white LED with color rendering index of 80 and correlated color temperature of 8715 K is obtained by combining the single CSS:0.05Ce^{3+}, 0.01Pr^{3+}, 0.3Mg^{2+} phosphor with a blue-emitting InGaN LED chip.

1. Introduction

White light emitting diodes (LEDs) are considered to be a promising candidate for future lighting systems because of their higher efficiency, longer lifetime, and lack of requirement for pollutants compared with conventional light sources such as incandescent lamps or fluorescent lamps.[1,2] Until now, the most widely used commercial white LEDs were fabricated by combining high performance blue-emitting InGaN chip with $Y_3Al_5O_{12}:Ce^{3+}$ (YAG:Ce^{3+}) yellow emitting aluminate garnet phosphor that exhibits an emission band peaking at 530 nm with a shoulder at 575 nm, originating from 5d→$^2F_{7/2}$, $^2F_{5/2}$ transitions of Ce^{3+}, respectively.[3,4] YAG:Ce^{3+} has a high converting efficiency, but the deficient red emitting component leads to the color rendering index (CRI) of the white LEDs below 80.[5,6]

To resolve this problem, the method of blending YAG:Ce^{3+} with red emitting phosphors has been proposed. Many studies have therefore been devoted to the development of high performance red phosphors, such as $M_2Si_5N_8:Eu^{2+}$ (M = Ca, Sr, Ba),[7] $CaAlSiN_3:Eu^{2+}$,[8] and $Lu_2CaMg_2Si_3O_{12}:Ce^{3+}$.[9] The drawback of phosphor blend is fluorescence reabsorption that results in loss of luminous efficiency. Hence, full color emitting single phase phosphors are expected. The attempt to enhance red emission components in YAG:Ce^{3+} was performed by co-doping Pr^{3+} on Y^{3+} site to generate a red emission line around 610 nm, originating from $^1D_2$→$^3H_4$ transitions of Pr^{3+} through Ce^{3+}→Pr^{3+} ET.[6] A new yellow-emitting $Ba_{0.93}Eu_{0.07}Al_2O_4$ phosphor with sufficient red component, very good thermal stability was also synthesized by Xufan Li *et al.* Warm-white emissions with correlated color temperature (CCT) < 4000 K and CRI > 80 were readily achieved when combining this phosphor with a blue light-emitting diode (440–470 nm).[10]

Recently, Yasuo Shimomura *et al.*[11] reported a novel green emitting silicate garnet phosphor $Ca_3Sc_2Si_3O_{12}:Ce^{3+}$ (CSS:Ce^{3+}) suitable for blue LED excitation. In this host lattices, Ce^{3+} substitution for the dodecahedral Ca^{2+} site is suggested based on the results of extended X-ray absorption fine structure (EXAFS) analysis. It was also found that the emission band appears to have a remarkable red shift if codoping Mg^{2+} to replace Sc^{3+}, being able to modify CSS:Ce^{3+} to be a yellow emitting phosphor $Ca_3(Sc_{2-b}Mg_b)Si_3O_{12}:Ce^{3+}$ ($0 \le b \le 1$).[12] In addition, vacuum ultraviolet spectroscopy of CSS doped with Pr^{3+} in Ca^{2+} site has been studied for searching for a novel fast emitting scintillator by Ivanovskikh *et al.*[13] The addition of Mg^{2+} in Sc^{3+} site is also performed to improve the properties of this novel fast emitting scintillator.[14]

In this paper, we investigate the energy transfer (ET) from Ce^{3+} to Pr^{3+} and the effect of addition of Mg^{2+} on the luminescence properties of phosphor CSS:Ce^{3+}, Pr^{3+}. A blue-based white LED with CRI of 80 and CCT of 8715 K is obtained by using the single phase CSS:0.05Ce^{3+}, 0.01Pr^{3+}, 0.3Mg^{2+} phosphor, demonstrating its potential application in white LEDs.

[a]*Key Laboratory of Luminescence and Application, Changchun Institute of Optics, Fine Mechanics and Physics, Chinese Academy of Sciences, Changchun, China. E-mail: zhangjh@ciomp.ac.cn; Tel: +86-431-8617-6317*
[b]*University of Chinese Academy of Sciences, Beijing 100039, P. R. China*

2. Experimental

2.1. Materials and synthesis

The phosphors $Ca_3Sc_2Si_3O_{12}$:0.05Ce^{3+}, xPr^{3+} (CSS:0.05Ce^{3+}, xPr^{3+}) (x = 0–0.06), $Ca_3(Sc_{2-y}Mg_y)Si_3O_{12}$:0.01$Pr^{3+}$ (CSS:0.01Pr^{3+}, yMg^{2+}), $Ca_3(Sc_{2-y}Mg_y)Si_3O_{12}$:0.05$Ce^{3+}$ (CSS:0.05Ce^{3+}, yMg^{2+}) and $Ca_3(Sc_{2-y}Mg_y)Si_3O_{12}$:0.05$Ce^{3+}$, 0.01$Pr^{3+}$ (CSS:0.05Ce^{3+}, 0.01Pr^{3+}, yMg^{2+}) (y = 0–0.3) were synthesized by conventional solid-state reaction. The constituent oxides or carbonates $CaCO_3$, Sc_2O_3, SiO_2, MgO, CeO_2, and $Pr(NO_3)_3$ were employed as the raw materials. The mixtures of raw materials were sintered in a tubular furnace at 1350 °C for 4 h in reductive atmosphere (5% H_2 + 95% N_2).

2.2. Measurements and characterization

The photoluminescence (PL) and photoluminescence excitation (PLE) spectra were measured using a FS920 spectrometer (Edinburgh Instruments, UK). The diffuse reflectance (DR) spectra were measured using HITACHI F-7000 spectrometer. The fluorescence decay curves of Ce^{3+} were measured by a FL920 Fluorescence Lifetime Spectrometer (Edinburgh Instruments, Livingston, UK) and a hydrogen flash lamp (nF900, Edinburgh Instruments). In the measurements of fluorescence decay of Pr^{3+}, an optical parametric oscillator (OPO) is used as an excitation source. The signal is detected by a Tektronix digital oscilloscope (TDS 3052). Powder X-ray diffraction (XRD) data were collected using Cu-Kα radiation (λ = 1.54056 Å) on a Bruker D8 Advance diffractometer. The chromaticity coordinates, CRI and the CCT of white LEDs were measured using Ocean Optics USB4000 Spectrometer.

3. Results and discussion

Fig. 1 shows the PLE and PL spectra for CSS:0.05Ce^{3+} (a), CSS:0.02Pr^{3+} (b) and CSS:0.05Ce^{3+}, 0.02Pr^{3+} (c). CSS:0.05Ce^{3+} exhibits a typical green PL band with a peak at 505 nm and a shoulder around 540 nm, originating from the transitions from 5d to $^2F_{5/2}$ and $^2F_{7/2}$ of Ce^{3+}, respectively.[11] Meanwhile, the PLE spectrum for the green emission exhibits an intense excitation band around 450 nm, well matching the emitting wavelength of the blue InGaN LEDs. The Pr^{3+} singly doped CSS exhibits a red emission around 610 nm, originating from $^1D_2 \rightarrow {}^3H_4$ transition of Pr^{3+}. The PLE spectrum for the red emission of Pr^{3+} includes two bands. The band in the range of 430 to 500 nm is attributed to the transitions from the $^3H_4$ ground state to the upper triply split ^3P_J (J = 0, 1, 2) levels and the $^1I_6$ level, and another band peaked around 285 nm is ascribed to the electronic transitions from the $^3H_4$ level to the $4f^15d$ band.[15,16] In CSS:0.05Ce^{3+}, 0.02Pr^{3+}, the PL spectrum upon Ce^{3+} excitation at 400 nm exhibits not only the Ce^{3+} emission band around 505 nm but also the Pr^{3+} emission around 610 nm, and the typical PLE band of Ce^{3+} accounts for the dominant part in the PLE spectrum around 450 nm by monitoring at 610 nm. These features prove that there is obvious ET from Ce^{3+} to Pr^{3+} in Ce^{3+} and Pr^{3+} co-doped sample. The occurrence of ET can be clearly understood as noticing the spectral overlap between the Ce^{3+} emission band in CSS:0.05Ce^{3+} and the Pr^{3+} excitation band in CSS:0.02Pr^{3+}.

Fig. 2 shows the normalized PL spectra for CSS:0.05Ce^{3+}, xPr^{3+} by 400 nm excitation. Considering that the excitation wavelength of 400 nm can only directly excite Ce^{3+} rather than Pr^{3+}, the excitation of Pr^{3+} must be performed completely

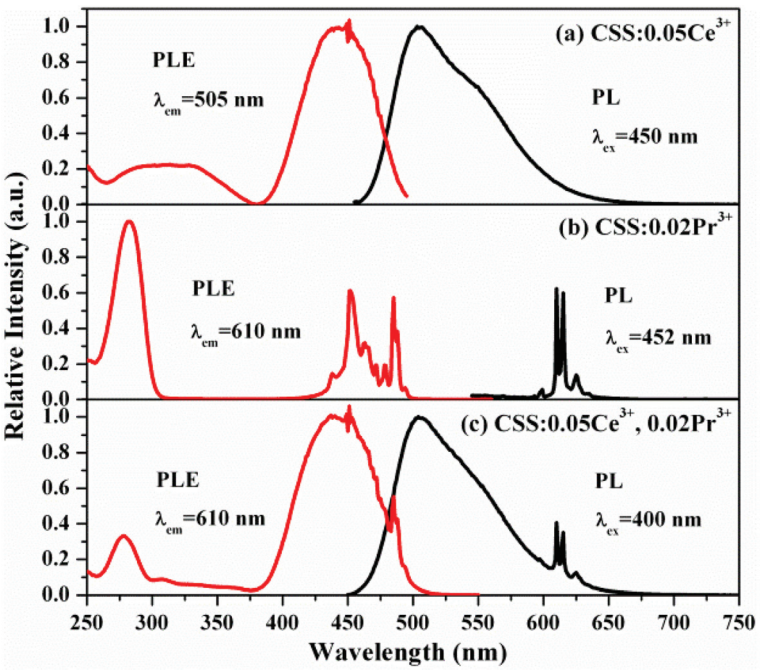

Fig. 1 PLE and PL spectra for CSS:0.05Ce^{3+} (a), CSS:0.02Pr^{3+} (b) and CSS:0.05Ce^{3+}, 0.02Pr^{3+} (c).

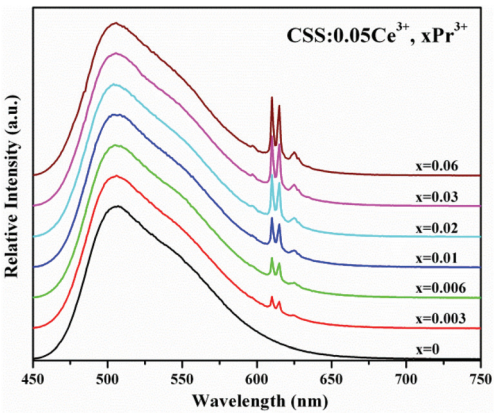

Fig. 2 Normalized PL spectra for CSS:0.05Ce^{3+}, xPr^{3+} under 400 nm excitation.

through Ce^{3+}→Pr^{3+} ET. It is observed that the intensity of Pr^{3+} emission obviously increases with increasing the nominal Pr^{3+} content in the raw material, reflecting the enhanced ET efficiency with increasing the concentration of Pr^{3+} in CSS. In contrast to the phenomena that remarkable concentration quenching takes place for Pr^{3+} concentration at 0.06 in $Y_3Al_5O_{12}$,[17] the intensity of Pr^{3+} emission continuously increases with increasing the Pr^{3+} content to 0.06 in the raw material of CSS, as shown in Fig. 2. Considering the fact that Ce^{3+} in CSS has a limited solubility around mole 1.1% due to the charge mismatch when Ce^{3+} substitutes for Ca^{2+}, as reported by Yasuo Shimomura *et al.*,[11] Pr^{3+} may meet the same situation. We therefore infer that the real concentration of Pr^{3+} incorporated in CSS lattices is lower than both the nominal concentration and the quenching concentration. This viewpoint is supported by the observation of slightly shortened Pr^{3+} $^1D_2$ lifetimes at higher concentrations, as shown in Fig. 3 (a). The decay curves of Pr^{3+} $^1D_2$ state for different Pr^{3+} nominal contents are measured by monitoring $^1D_2$→$^3H_5$ emission of Pr^{3+} at 714 nm upon $^3H_4$→$^1D_2$ pulsed excitation at 610 nm. In addition, the fluorescence decay curves of Ce^{3+} monitored at 505 nm upon pulsed excitation at 450 nm are presented in Fig. 3(b). Compared with fluorescence lifetime (69 ns) of Ce^{3+} in the absence of Pr^{3+}, the tiny variation about that of Ce^{3+} in presence of Pr^{3+} indicates the ET efficiency from Ce^{3+} to Pr^{3+} is very limited due to low Pr^{3+} concentration in CSS. The longer average distance between Ce^{3+} and Pr^{3+} results in a weak interaction between them, so the ET from Ce^{3+} to Pr^{3+} is not very efficient.

In order to explore the approach for enhancing the Pr^{3+} concentration in CSS, we have tentatively prepared CSS:0.05Ce^{3+}, 0.01Pr^{3+}, yMg^{2+} with a fixed nominal Pr^{3+} content at 0.01 and various nominal Mg^{2+} content y from 0 to 0.3, in which Mg^{2+} is incorporated into CSS by substituting the Sc^{3+} site due to the ionic radius of Mg^{2+} being close to that of Sc^{3+}.[12]

Fig. 4 shows the XRD patterns for the phosphors with nominal compositions of $Ca_{2.94}Sc_{2-y}Mg_ySi_3O_{12}$:0.05$Ce^{3+}$, 0.01$Pr^{3+}$ (y = 0–0.3). The primary phase in all of these samples is CSS garnets (JCPDF no. 72-1969) with a few by-products of Sc_2O_3 phase (JCPDF no. 74-1210) and $Ca_3(Si_3O_9)$ phase (JCPDF no. 74-0874). In addition, when the nominal content of Mg^{2+} reaches to 0.3 in the raw material, a by-product $Ca_2MgSi_2O_7$ phase (▼) (JCPDF no. 35-0592) emerges in the sample due to the fact that excessive Mg^{2+} in the raw material cannot be incorporated into the CSS garnet phosphor. Fortunately, the by-products do not affect the luminescence properties of the phosphor.[12]

Fig. 5 shows the PL spectra for CSS:0.05Ce^{3+}, 0.01Pr^{3+}, yMg^{2+} under 400 nm excitation (a) and CSS:0.01Pr^{3+}, yMg^{2+} under 452 nm excitation (b). The PL spectra of Ce^{3+} in the phosphors containing Mg^{2+} are moved toward longer wavelength with increasing Mg^{2+} content in the raw material. As reported by Yasuo Shimomura *et al.*, this phenomenon is

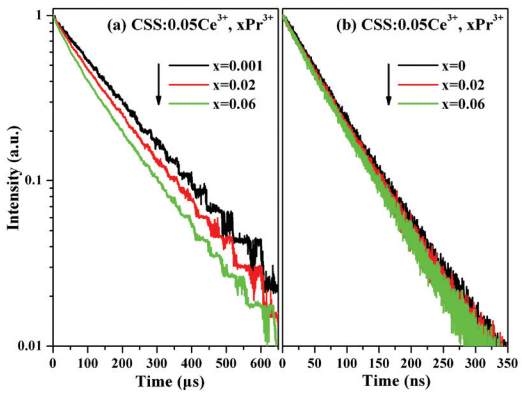

Fig. 3 Photoluminescence decay curves of Pr^{3+} (excited at 610 nm, monitored at 714 nm) (a) and Ce^{3+} (excited at 450 nm, monitored at 505 nm) (b) in CSS:0.05Ce^{3+}, xPr^{3+}.

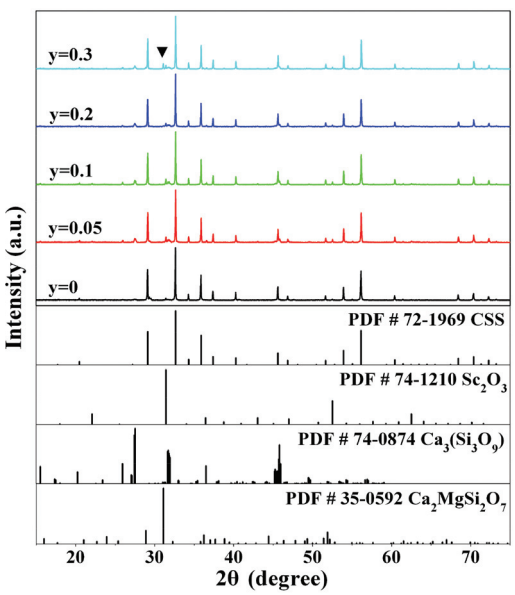

Fig. 4 XRD patterns for phosphors with nominal compositions of $Ca_{2.94}Sc_{2-y}Mg_ySi_3O_{12}$:0.05$Ce^{3+}$, 0.01$Pr^{3+}$ (y = 0–0.3).

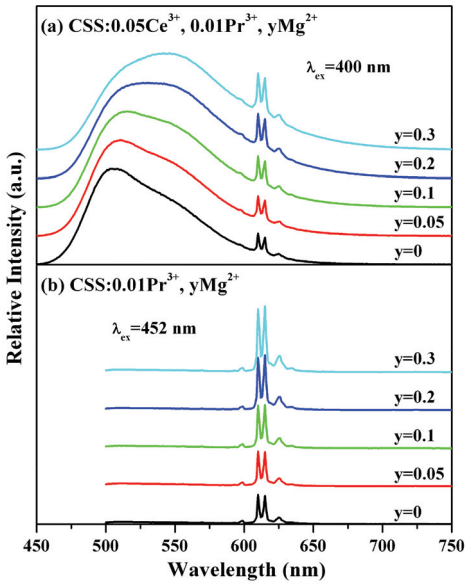

Fig. 5 PL spectra for CSS:0.05Ce^{3+}, 0.01Pr^{3+}, $y$$Mg^{2+}$ under 400 nm excitation (a), and CSS:0.01Pr^{3+}, $y$$Mg^{2+}$ under 452 nm excitation (b).

likely caused by the increase in amount of the activator.[12] Some interaction among the activators probably modified the luminescence characteristics. This conclusion can be also demonstrated in the DR spectra for CSS:0.05Ce^{3+}, $y$$Mg^{2+}$ (Fig. 6(a)), in which the absorption around 450 nm that is attributed to the typical 4f→5d transition of Ce^{3+} in CSS enhances with increasing Mg^{2+} content, indicating that Mg^{2+} substitution for Sc^{3+} can promote Ce^{3+} incorporation into CSS lattices by compensating the charge mismatch between Ce^{3+} and Ca^{2+}.

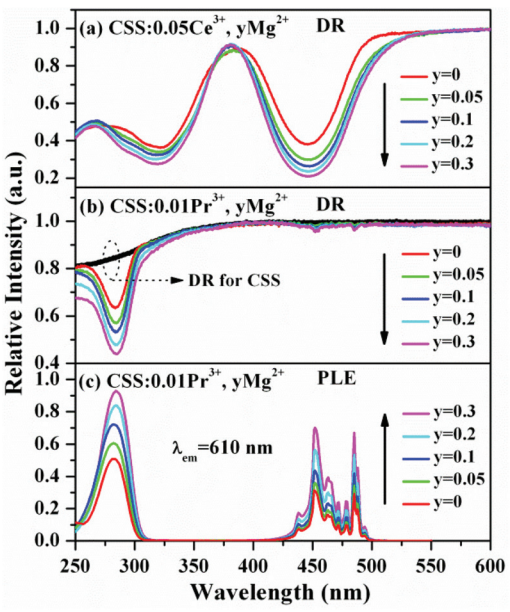

Fig. 6 DR spectra for CSS:0.05Ce^{3+}, $y$$Mg^{2+}$ (a), CSS:0.01Pr^{3+}, $y$$Mg^{2+}$ (b) and PLE spectra for CSS:0.01Pr^{3+}, $y$$Mg^{2+}$ (c).

In contrast, the PL spectra of Pr^{3+} in these samples are located around 610 nm without any red shift with increasing Mg^{2+} content, due to the Pr^{3+} emission around 610 nm originating from $^1D_2 \rightarrow {}^3H_4$ transition which is hardly affected by the local environment. Nonetheless, the intensity of Pr^{3+} emission around 610 nm is markedly enhanced in the spectra for not only CSS:0.05Ce^{3+}, 0.01Pr^{3+}, $y$$Mg^{2+}$ but also CSS:0.01Pr^{3+}, $y$$Mg^{2+}$ by increasing Mg^{2+} content. In view of the effect of Mg^{2+} in CSS:0.05Ce^{3+}, $y$$Mg^{2+}$, we infer that the enhancement of Pr^{3+} emission is ascribed to the increasing Pr^{3+} concentration in CSS, Mg^{2+} substitution for Sc^{3+} can compensate the residual positive charge caused by Pr^{3+} substitution for Ca^{2+}.

Fig. 6(b) and 6(c) show the DR spectra and PLE spectra (λ_{em} = 610 nm) for CSS:0.01Pr^{3+}, $y$$Mg^{2+}$, respectively. The bold black line in Fig. 6(b) represents the DR spectrum for undoped CSS. The slender absorptions in the range of 430 to 500 nm are attributed to the transitions of Pr^{3+} from the $^3H_4$ ground state to the upper triply split ^3P_J (J = 0, 1, 2) levels and the $^1I_6$ level. The absorption around 285 nm is ascribed to the electronic transition of Pr^{3+} from the $^3H_4$ level to the $4f^15d$ band.[15,16] With increasing Mg^{2+} content in the raw material, the absorptions, which are correlated to the amount of Pr^{3+} in CSS, are gradually enhanced, indicating that the Pr^{3+} concentration is increased by the incorporation of Mg^{2+} into CSS lattices. This conclusion accords with our previous inference. The PLE bands (λ_{em} = 610 nm) for CSS:0.01Pr^{3+}, $y$$Mg^{2+}$ are also located around 285 nm and in the range of 430 to 500 nm, well consistent with their DR bands, as shown in Fig. 6(c).

To evaluate the chromaticity characteristics of white light generated from our present phosphor under blue light excitation, a white LED is fabricated. As shown in Fig. 7, when the single phosphor with nominal composition of CSS:0.05Ce^{3+}, 0.01Pr^{3+}, 0.3Mg^{2+} is excited by a blue InGaN LED (450 nm) chip, a white LED with CRI of 80, CCT of 8715 K and chromaticity coordinates of (0.28, 0.32) is obtained at the forward current of 20 mA. The results of this work demonstrate the potential application of the single CSS:0.05Ce^{3+}, 0.01Pr^{3+},

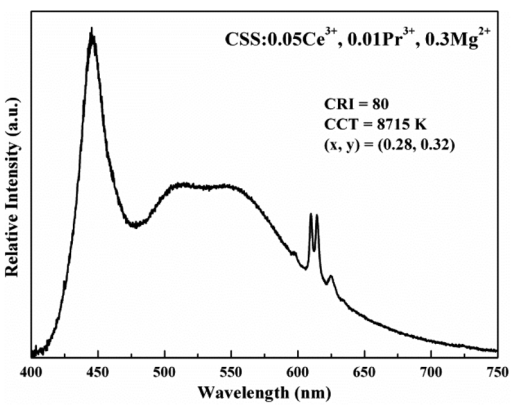

Fig. 7 Emission spectrum for the white LED fabricated using the single phosphor with nominal composition of CSS:0.05Ce^{3+}, 0.01Pr^{3+}, 0.3Mg^{2+} and an InGaN LED (λ_{ex} = 450 nm) chip. The current is 20 mA.

$0.3Mg^{2+}$ phosphor in blue-based white LEDs. However, this white LED needs more red emission components to be excellent lighting source. In order to improve the performance of this white LED to obtain ideal lighting source with higher CRI and lower CCT, further exploration to enhance the red emission of this phosphor is necessary.

4. Conclusions

In summary, we investigated the $Ce^{3+}\rightarrow Pr^{3+}$ ET in the silicate garnet CSS. The luminescence spectra exhibit a red Pr^{3+} emission around 610 nm through the $Ce^{3+}\rightarrow Pr^{3+}$ ET upon excitation at 400 nm. The intensity of Pr^{3+} emission continuously increases with increasing the Pr^{3+} content to 0.06 in the raw material, due to the limited increasing concentration of Pr^{3+} in CSS enhancing the ET efficiency from Ce^{3+} to Pr^{3+}. The addition of Mg^{2+} can not only increase Ce^{3+} concentration in CSS to make PL spectra move toward longer wavelength, but also promote Pr^{3+} incorporation into CSS lattices to enhance the Pr^{3+} emission. The luminescence spectra of CSS:$0.05Ce^{3+}$, $0.01Pr^{3+}$ containing Mg^{2+} were modified to contain enriched longer wavelength emissive components so as to generate white light. A white LED with CRI of 80, CCT of 8715 K and chromaticity coordinates of (0.28, 0.32) was fabricated by combining the single CSS:$0.05Ce^{3+}$, $0.01Pr^{3+}$, $0.3Mg^{2+}$ phosphor with an InGaN LED (450 nm) chip. Our works demonstrate the promising application of this phosphor in blue-based white LEDs. In order to improve the performance of this white LED to obtain ideal lighting source, further exploration is needed to enrich the red emission of this phosphor.

Acknowledgements

This work is financially supported by the National Natural Science Foundation of China (51172226, 61275055, 11274007 and 11174278) and the Natural Science Foundation of Jilin province (201205024, 20140101169JC).

Notes and references

1 S. Nakamura, T. Mukai and M. Senoh, *Appl. Phys. Lett.*, 1994, **64**, 1687.
2 E. F. Schubert and J. K. Kim, *Science*, 2005, **308**, 1274.
3 K. Bando, K. Sakano, Y. Noguchi and Y. Shimizu, *J. Light Visual Environ.*, 1998, **22**, 2.
4 G. Blasse and A. Bril, *Appl. Phys. Lett.*, 1967, **11**, 53.
5 Y. Chen, M. Gong, G. Wang and Q. Su, *Appl. Phys. Lett.*, 2007, **91**, 071117.
6 H. S. Jang, W. B. Im, D. C. Lee, D. Y. Jeon and S. S. Kim, *J. Lumin.*, 2007, **126**, 371.
7 Y. Q. Li, J. E. J. van Steen, J. W. H. van Krevel, G. Botty, A. C. A. Delsing, F. J. DiSalvo, G. de With and H. T. Hintzen, *J. Alloys Compd.*, 2006, **417**, 273.
8 K. Uheda, N. Hirosaki, Y. Yamamoto, A. Naito, T. Nakajima and H. Yamamoto, *Electrochem. Solid-State Lett.*, 2006, **9**, H22.
9 A. A. Setlur, W. J. Heward, Y. Gao, A. M. Srivastava, R. G. Chandran and M. V. Shankar, *Chem. Mater.*, 2006, **18**, 3314.
10 X. F. Li, J. D. Budai, F. Liu, J. Y. Howe, J. H. Zhang, X. J. Wang, Z. J. Gu, C. J. Sun, R. S. Meltzer and Z. W. Pan, *Light: Sci. Appl.*, 2013, **2**, e50.
11 Y. Shimomura, T. Honma, M. Shigeiwa, T. Akai, K. Okamoto and N. Kijima, *J. Electrochem. Soc.*, 2007, **154**, J35.
12 Y. Shimomura, T. Kurushima, M. Shigeiwa and N. Kijima, *J. Electrochem. Soc.*, 2008, **155**, J45.
13 K. V. Ivanovskikh, A. Meijerink, F. Piccinelli, A. Speghini, E. I. Zinin, C. Ronda and M. Bettinelli, *J. Lumin.*, 2010, **130**, 893.
14 K. V. Ianovskikh, A. Meijerink, F. Piccinelli, A. Speghini, C. Ronda and M. Bettinelli, *ECS J. Solid State Sci. Technol.*, 2012, **1**, R127.
15 R. Marin, G. Sponchia, P. Riello, R. Sulcis and F. Enrichi, *J. Nanopart. Res.*, 2012, **14**, 886.
16 R. Piramidowicz, K. Ławniczuk, M. Nakielska, J. Sarnecki and M. Malinowski, *J. Lumin.*, 2008, **128**, 708.
17 L. Wang, X. Zhang, Z. D. Hao, Y. S. Luo, J. H. Zhang and X. J. Wang, *J. Appl. Phys.*, 2010, **108**, 093515.

